Prediction of Two-Photon Absorption Properties for Organic Chromophores Using Time-Dependent Density-Functional Theory

Artëm Masunov and Sergei Tretiak*

Theoretical Division, Los Alamos National Laboratory, Los Alamos, New Mexico 87545

Received: August 22, 2003; In Final Form: October 28, 2003

In this benchmark study, time-dependent density-functional theory (TDDFT) is applied to calculate one- and two-photon absorption spectra (related to linear and third-order optical responses, respectively) in a series of large donor−acceptor substituted conjugated molecules. Calculated excitation energies corresponding to one- and two-photon-absorption maxima are found to be in excellent agreement with experiment. The evaluated two-photon-absorption cross sections agree with experimental data as well. We conclude that the TDDFT approach is a numerically efficient method for quantitative calculations of resonant nonlinear polarizabilities in large organic chromophores.

I. Introduction

Two-photon absorption (TPA) involves electronic excitation of a molecule induced by a pair of photons of the same or different energy. Unlike one-photon absorption (OPA), TPA is quadratically proportional to the intensity of the incident light, and hence, by focusing the beam, one can precisely localize TPA in a small volume up to one wavelength in size deep inside the bulk of the material. This property of TPA holds great promise for many useful applications[1] such as manufacturing of optoelectronic logical circuits[2] and three-dimensional optical data storage,[3−6] optical power limiting,[7] upconversion lasing,[8] in vivo imaging of biological tissues,[9,10] and photodynamic therapy.[11] However, to minimize photodamage, one has to utilize lasers of lower intensity. Existing materials do not absorb enough at low intensities, and this makes synthesis of new materials with large TPA cross sections an important goal. In particular, an accurate theoretical prediction of TPA properties (both frequencies and cross sections) is necessary for the rational design of chromophores with enhanced nonlinear optical response.

Until very recently, most known organic molecules possessed low TPA cross sections, on the order of 10s of GM (Göppert−Mayers, 1 GM = 10^{-50} cm^4 s). Recent advances in molecular design and modeling by Webb,[12,13] Reinhardt,[14,15] Perry,[16−18] and others have led to key design strategies linking two-photon-absorbing properties to the molecular structure. Enhanced nonlinear properties in these functional materials result from long-range collective electronic "communications" (coherence and charge transport).[19] Therefore, there is a clear need for quantitative computational approaches able to calculate molecular clusters with hundreds of atoms in size and to fully investigate electronic phenomena and predict trends.

While post-Hartree−Fock (HF) ab initio methods, such as MR−CI (multireference configuration interaction) and CASPT2 (complete active space with perturbation theory correction to the second order), provide an accurate description of the electronic transitions in principle, they are prohibitively expensive when applied to the molecules of practical interest. Semiempirical methods, on the other hand, are usually parametrized for the ground state (e.g., Austin Model 1 (AM1)) and (at most) the excited states active in the linear spectroscopy (e.g., the intermediate neglect of differential overlap/spectroscopy (INDO/S) model, fitted to reproduce UV−vis absorption spectra at the CI singles (CIS) level). These models are often in error when applied to the two-photon transitions where higher excited-state energy levels are involved and double excitations are important. Methods including higher-order correlations are computationally expensive and often result in the overcorrelated ground-state wave function.[16,18] In addition, size consistency is not guaranteed and special care needs to be taken when choosing the right configurations.[20−22]

Random phase approximation (RPA) theory, also known as the time-dependent Hartree−Fock (TDHF) method,[23] was shown to be an affordable way to treat electronic spectroscopy of large molecules.[24] However, systematic deviations from the experimental data[25] remain in the description of the correlated electronic states. Here we propose to use an adiabatic TDDFT approach[26] for calculation of TPA properties in large organic molecules. We expect TDDFT to perform well in TPA calculations based on the success of this method in the description of the excited states. TDDFT was shown to be superior to both semiempirical (ZINDO and PM3/S)[27] and low-level ab initio (CIS and TDHF)[28,29] results in predicting electronic excitations into the valence states. In particular, TDDFT calculates relatively well even states with significant double excitation character such as A_g states in centrosymmetric molecules.[30] Higher-lying Rydberg states are also well reproduced by TDDFT if asymptotic corrections to the standard GGA functional are made and large basis sets are used.[31,28] Typical hybrid functionals, such as the B3LYP model, provide the best accuracy.[32] In addition, the extensions of TDDFT to second- and third-order properties have been explored in several studies[33−35] and, in particular, for TPA properties in small molecules.[36]

Recently we have shown that the density matrix formulation of the time-dependent Kohn−Sham equations[33,37,38] allows treatment of adiabatic TDDFT on the same footing as the TDHF theory to an arbitrary order in the external perturbation.[39] This allows us to obtain closed expressions for frequency-dependent optical polarizabilities up to the third order in the driving field.[39] In this article, we use these equations for computing the third-order optical response and, subsequently, TPA energies and

* Corresponding author. E-mail: serg@lanl.gov.

10.1021/jp036513k CCC: $27.50
Published on Web 12/18/2003

cross sections in the extended molecular systems. As a benchmark for our TDDFT calculations, we selected recently published extensive experimental and theoretical studies of stilbene and bis(styryl)benzene derivatives.[16−18,40,41]

II. Theoretical Methodology

The two-photon-absorption cross section σ is related to the imaginary part of the third-order polarizability γ as[16−18,40,41]

$$\sigma_{\mathrm{TPA}}(\omega) = \frac{4\pi^2\hbar\omega^2}{n^2c^2} L^4 Im\langle\gamma(\omega,\omega,-\omega)\rangle \qquad (2.1)$$

where $\hbar$ is Plank's constant, c is the speed of light, n is the refractive index of the media, L is the local field factor, and

$$\langle\gamma\rangle = \frac{1}{15}(3\sum_i \gamma_{iiii} + \sum_{i\neq j}(\gamma_{iijj} + \gamma_{ijji} + \gamma_{ijij})) \qquad (2.2)$$

is the average over all orientations, where indices i and j refer to spatial directions x, y, and z.[42]

Traditional evaluation of the third-order polarizability using the perturbative sum-over-state (SOS) approach[43,44] requires ground- and excited-state energies, state dipoles, and transition dipoles. However, the manifold of contributing states and transition dipole moments between the excited states are not available from linear response theory (see a detailed discussion in ref 39). Alternative expressions for the frequency-dependent polarizabilities have been recently derived specifically for TDHF and TDDFT approaches.[23,39] These equations require only quantities that can be obtained from linear response theory and the corresponding functional derivatives in the TDDFT method.

In particular, the third-order polarizability corresponding to TPA eqs 2.1 and 2.2 can be calculated using an eight-term expression symmetrized with respect to ω_1, ω_2, and ω_3 permutations[23,39]

$$\gamma_{ijkl}(\omega_1{=}\omega,\omega_2{=}\omega,\omega_3{=}-\omega) = \frac{e^4}{6\hbar^3}\sum_{\omega_1,\omega_2,\omega_3}^{\mathrm{perm}}(\gamma_{ijkl}^{(\mathrm{I})} + \gamma_{ijkl}^{(\mathrm{II})} + ... + \gamma_{ijkl}^{(\mathrm{VIII})}) \qquad (2.3)$$

where

$$\gamma_{ijkl}^{(\mathrm{I})} = \sum_{\alpha\beta\gamma}\frac{\mu_{-\alpha\beta}^{(j)}\mu_{-\beta\gamma}^{(k)}\mu_{\alpha}^{(i)}\mu_{-\gamma}^{(l)}S_\alpha S_\beta S_\gamma}{(\Omega_\alpha-\omega_1-\omega_2-\omega_3)(\Omega_\beta-\omega_2-\omega_3)(\Omega_\gamma-\omega_3)} \qquad (2.4)$$

$$\gamma_{ijkl}^{(\mathrm{II})} = \sum_{\alpha\beta\gamma\delta}\frac{-\mu_{-\alpha\beta}^{(j)}V_{-\beta\gamma\delta}\mu_{\alpha}^{(i)}\mu_{-\gamma}^{(k)}\mu_{-\delta}^{(l)}S_\alpha S_\beta S_\gamma S_\delta}{(\Omega_\alpha-\omega_1-\omega_2-\omega_3)(\Omega_\beta-\omega_2-\omega_3)(\Omega_\gamma-\omega_2)(\Omega_\delta-\omega_3)} \qquad (2.5)$$

$$\gamma_{ijkl}^{(\mathrm{III})} = \sum_{\alpha\beta\gamma}\frac{\mu_{-\alpha\beta\gamma}^{(j)}\mu_{\alpha}^{(i)}\mu_{-\beta}^{(k)}\mu_{-\gamma}^{(l)}S_\alpha S_\beta S_\gamma}{(\Omega_\alpha-\omega_1-\omega_2-\omega_3)(\Omega_\beta-\omega_2-\omega_3)(\Omega_\gamma-\omega_3)} \qquad (2.6)$$

$$\gamma_{ijkl}^{(\mathrm{IV})} = \sum_{\alpha\beta\gamma\delta}\frac{-2V_{-\alpha\beta\gamma}\mu_{-\gamma\delta}^{(k)}\mu_{\alpha}^{(i)}\mu_{-\beta}^{(j)}\mu_{-\delta}^{(l)}S_\alpha S_\beta S_\gamma S_\delta}{(\Omega_\alpha-\omega_1-\omega_2-\omega_3)(\Omega_\beta-\omega_1)(\Omega_\gamma-\omega_2-\omega_3)(\Omega_\delta-\omega_3)} \qquad (2.7)$$

$$\gamma_{ijkl}^{(\mathrm{V})} = \sum_{\alpha\beta\gamma\delta\eta}\frac{2V_{-\alpha\beta\gamma}V_{-\gamma\delta\eta}\mu_{\alpha}^{(i)}\mu_{-\beta}^{(j)}\mu_{-\delta}^{(k)}\mu_{-\eta}^{(l)}S_\alpha S_\beta S_\gamma S_\delta S_\eta}{(\Omega_\alpha-\omega_1-\omega_2-\omega_3)(\Omega_\beta-\omega_1)(\Omega_\gamma-\omega_2-\omega_3)(\Omega_\delta-\omega_2)(\Omega_\eta-\omega_3)} \qquad (2.8)$$

$$\gamma_{ijkl}^{(\mathrm{VI})} = \sum_{\alpha\beta\gamma\delta}\frac{-V_{-\alpha\beta\gamma\delta}\mu_{\alpha}^{(i)}\mu_{-\beta}^{(j)}\mu_{-\gamma}^{(k)}\mu_{-\delta}^{(l)}S_\alpha S_\beta S_\gamma S_\delta}{(\Omega_\alpha-\omega_1-\omega_2-\omega_3)(\Omega_\beta-\omega_1)(\Omega_\gamma-\omega_2)(\Omega_\delta-\omega_3)} \qquad (2.9)$$

$$\gamma_{ijkl}^{(\mathrm{VII})} = \sum_{\alpha\beta\gamma}\frac{\mu_{\alpha\beta}^{(i)}\mu_{-\beta\gamma}^{(k)}\mu_{-\alpha}^{(j)}\mu_{-\gamma}^{(l)}S_\alpha S_\beta S_\gamma}{(\Omega_\alpha-\omega_1)(\Omega_\beta-\omega_2-\omega_3)(\Omega_\gamma-\omega_3)} \qquad (2.10)$$

$$\gamma_{ijkl}^{(\mathrm{VIII})} = \sum_{\alpha\beta\gamma\delta}\frac{-\mu_{\alpha\beta}^{(i)}V_{-\beta\gamma\delta}\mu_{-\alpha}^{(j)}\mu_{-\gamma}^{(k)}\mu_{-\delta}^{(l)}S_\alpha S_\beta S_\gamma S_\delta}{(\Omega_\alpha-\omega_1)(\Omega_\beta-\omega_2-\omega_3)(\Omega_\gamma-\omega_2)(\Omega_\delta-\omega_3)} \qquad (2.11)$$

Here $S_\alpha = \mathrm{sign}(\alpha)$, indices $s = i, j, k, l$ label the spatial directions (x, y, and z), indices $\nu = \alpha, \beta, \gamma, \delta, \eta = -M, ..., M$ run over the excited states, and Ω_ν are excitation energies obtained from linear response theory by diagonalization of the Liouville operator

$$L\xi_\nu = \Omega_\nu\xi_\nu \quad L\xi_\nu^\dagger = -\Omega_\nu\xi_\nu^\dagger \quad \nu = 1, ..., M \qquad (2.12)$$

which eigenvectors (transition densities ξ_ν) come in conjugated pairs.[26,23] We assume that Ω_ν is positive (negative) for all $\nu > 0$ ($\nu < 0$) according to the convention $\Omega_{-\nu} = -\Omega_\nu$. The other variables[39]

$$\mu_\alpha^{(s)} = Tr(\mu^{(s)}\xi_\alpha) \qquad (2.13)$$

$$\mu_{\alpha\beta}^{(s)} = \sum_{\alpha\beta}^{\mathrm{perm}} Tr(\mu^{(s)}(I-2\bar{\rho})\xi_\alpha\xi_\beta) \qquad (2.14)$$

$$\mu_{\alpha\beta\gamma}^{(s)} = -\frac{1}{3}\sum_{\alpha\beta\gamma}^{\mathrm{perm}} Tr(\mu^{(s)}\xi_\alpha\xi_\beta\xi_\gamma) \qquad (2.15)$$

$$V_{\alpha\beta\gamma} = \frac{1}{2}\sum_{\alpha\beta\gamma}^{\mathrm{perm}} Tr((I-2\bar{\rho})\xi_\alpha\xi_\beta\tilde{V}(\xi_\gamma)) + \frac{1}{6}\sum_{\alpha\beta\gamma}^{\mathrm{perm}} Tr(\xi_\alpha v^{(2)}(\xi_\beta,\xi_\gamma)) \qquad (2.16)$$

$$V_{\alpha\beta\gamma\delta} = \frac{1}{12}\sum_{\alpha\beta\gamma\delta}^{\mathrm{perm}} Tr((I-2\bar{\rho})\xi_\alpha\xi_\beta\tilde{V}((I-2\bar{\rho})\xi_\gamma\xi_\delta)) - \frac{1}{12}\sum_{\alpha\beta\gamma\delta}^{\mathrm{perm}} Tr(\xi_\alpha\xi_\beta\xi_\gamma\tilde{V}(\xi_\delta)) + \frac{1}{12}\sum_{\alpha\beta\gamma\delta}^{\mathrm{perm}} Tr((I-2\bar{\rho})\xi_\alpha\xi_\beta v^{(2)}(\xi_\gamma,\xi_\delta)) + \frac{1}{12}\sum_{\alpha\beta\gamma\delta}^{\mathrm{perm}} Tr(\xi_\alpha v^{(2)}(((I-2\bar{\rho})\xi_\beta\xi_\gamma),\xi_\delta)) + \frac{1}{24}\sum_{\alpha\beta\gamma\delta}^{\mathrm{perm}} Tr(\xi_\alpha v^{(3)}(\xi_\beta,\xi_\gamma,\xi_\delta)) \qquad (2.17)$$

are tensors symmetrized with respect to all permutations of their indices (α, β, γ, δ, η) which describe coupling among the excited states mediated by Coulomb V and dipole μ interactions. Here $\mu^{(s)}$ is the dipole matrix for s-spatial direction, $\bar{\rho}$ is the ground-state density matrix, and I is a unit matrix. These are $K \times K$ matrixes in the orthonormal finite basis set of size K. The Coulomb exchange-correlation operator $\tilde{V}$ is defined as

$$\tilde{V}_{pq\sigma}(\xi) = \sum_{mn\sigma'} ((pq\sigma|mn\sigma')\xi_{mn\sigma'} - c_x(pm\sigma|qn\sigma)\xi_{mn\sigma}\delta_{\sigma\sigma'}) + \sum_{mn\sigma'} f_{pq\sigma,mn\sigma'}\xi_{mn\sigma'} \quad (2.18)$$

where $(pq\sigma|mn\sigma')$ denotes the two-electron integrals (indices p, q, m, n, and σ refer to the orbitals spatial and spin indices, respectively). Becke's mixing parameter c_x allows the introduction of the HF exchange and the construction of hybrid functionals.[45,46] $f_{pq\sigma,mn\sigma'}$ is the matrix element of the kernel corresponding to the functional derivative[26,47]

$$f_{\sigma\sigma'}(\mathbf{r},\mathbf{r}') = \frac{\delta^2 E^{xc}}{\delta n_\sigma(\mathbf{r})\delta n_{\sigma'}(\mathbf{r}')} \quad (2.19)$$

Here $E^{xc}[n]$ is an exchange-correlation functional of the charge density $n(\mathbf{r})$. Finally, the expressions for $v^{(2)}$ and $v^{(3)}$ are quadratic and cubic in ξ, respectively,[39] and depend on the third- and fourth-order functional derivatives that are currently being coded into some modern quantum-chemical packages primarily for implementing the analytic derivative technique in TDDFT.[47]

III. Computational Approach

For the practical implementation of this methodology, we used the Gaussian 98 package[48] to calculate the linear response in adiabatic TDDFT by solving an eigenproblem (2.12) and, subsequently, to print the excitation energies Ω_ν, transition densities ξ_ν, dipole matrixes $\mu^{(s)}$, and relevant Coulomb exchange-interaction matrixes $\tilde{V}(\xi_\nu)$ and $\tilde{V}((1/2)((\xi_\beta, \bar{\rho}),\xi_\alpha))$ defined by eq 2.18. To calculate the TPA frequencies and cross-section magnitudes, we utilize the collective electronic oscillator (CEO) program which computes first-, second-, and third-order responses in various regimes using the TDHF approach combined with the semiempirical Hamiltonian models.[23] Minor code modifications were required to interface the CEO with TDDFT data printout since both TDHF and TDDFT methods share the same mathematical description for the excited-state electronic structure.[39]

In our calculations, terms containing $v^{(2)}$ and $v^{(3)}$ in eqs 16 and 17 have been neglected since the appropriate functional derivatives are not yet available in the Gaussian suit.[48] We believe that these quantities will have a minor impact on the nonlinear polarizability magnitudes. In fact, as we show later in this paper, the Coulomb operators on the cross densities $\tilde{V}((1/2)((\xi_\beta, \bar{\rho}),\xi_\alpha))$ have negligible effect on the TPA cross sections. In practice, terms containing $v^{(2)}$ and $v^{(3)}$ are straightforward to implement into our code once the corresponding functional derivatives become available in the quantum-chemical codes. In section IV.C, we test the effect of various approximations in the third-order polarizability expression (2.3−2.11) to identify the major contributions.

The OPA and TPA properties of stilbene and bis(styryl)-benzene derivatives have been a subject of extensive experimental studies.[16−18] These molecular structures are shown on Figure 1. In this article, we use the experimental data to benchmark the accuracy of the TDDFT approach for OPA and TPA properties. All quantum chemical calculations were performed using Gaussian 98.[48] Unless stated otherwise, the 6-31G basis set was used for all calculations. For the DFT computations, we employed the B3LYP functional, which is the most commonly used and, arguably, the most accurate density functional in quantum chemistry. The geometry was optimized at the HF and B3LYP levels. The solvation effects were neglected. The optimized geometry was then used to carry out the TDDFT/B3LYP calculations.

Molecular structures used in the calculations (Figure 1) differ from those studied experimentally[16−18] as follows: the alkyl groups (butyl and dodecyl) and terminal phenyl rings in diphenylamino groups were replaced with the methyl groups. Some experimental data are available for both diphenylamino and dialkylamino derivatives. To distinguish them, we use letter **a** (**2a**, **3a**, etc.) for the molecules with the diphenylamino groups. All molecular geometries were optimized starting from the conformations analogous to geometries found in the crystal structures of **6a** and **11a**,[18] which means C_2 symmetry for molecules **1**, **2**, and **2a**, and C_i symmetry for the others. Molecular geometries were optimized in these symmetry groups, as well as in planar C_{2h} symmetry.

IV. Results and Discussions

A. The Effects of Molecular Geometry. Even the most accurate electronic structure method will fail if the input molecular geometry is not accurate. The effect of the input molecular geometries on the calculated TPA properties appears to be significant. The molecules in question are conjugated molecules, where typically two structural factors have a major impact on the electronic properties. The bond length alternation (BLA) parameter, defined as the difference in length between the single and double bonds (r(C—C) − r(C═C))[49] reflects the degree of an uneven distribution of the π electrons over the bonds (Peierls distortion). Additionally, the torsional disorder (nonplanarity) defined as the deviation of the torsional angle around the single bond from 180 degrees affects the delocalization of the π-electron system as well. Both parameters depend on the chemical substituents, solvent, and the other environmental factors. For instance, it has been reported[50] that the change from planar to twisted AM1 optimized geometry (nonplanarity of 25°) and the change in BLA from 0.075 to 0.090 Å for the molecule **11** mediated by approaching point charges increase the transition energy by 0.5 eV and decrease the TPA cross section 2-fold. In another family of molecules, however, the calculated TPA cross sections[51] increase upon twisting the molecule by 80° from the planar geometry.

It was shown that several DFT functionals yield planar optimal geometries for the unsubstituted stilbene, unlike the other methods, where nonplanarity increases when going from AM1 to HF and to MP2 (Møller−Plesset perturbation theory).[52] The BLA parameter can also vary from 0.15 Å in HF to 0.11 Å in AM1, MP2, and B3LYP methods. These results show a requirement for a careful choice of the geometry optimization method.

Unfortunately, the comparison of molecular geometries with experimental data is not straightforward. The nonplanarity of *trans*-stilbene (compound **1** in Figure 1) was a subject of debate. Even though the molecule appears to be almost planar in crystal at the room temperature, this is an artifact of positional disorder and pedal motion.[53] Even when the disorder is not detected, the average length of the central bond and nonplanarity may

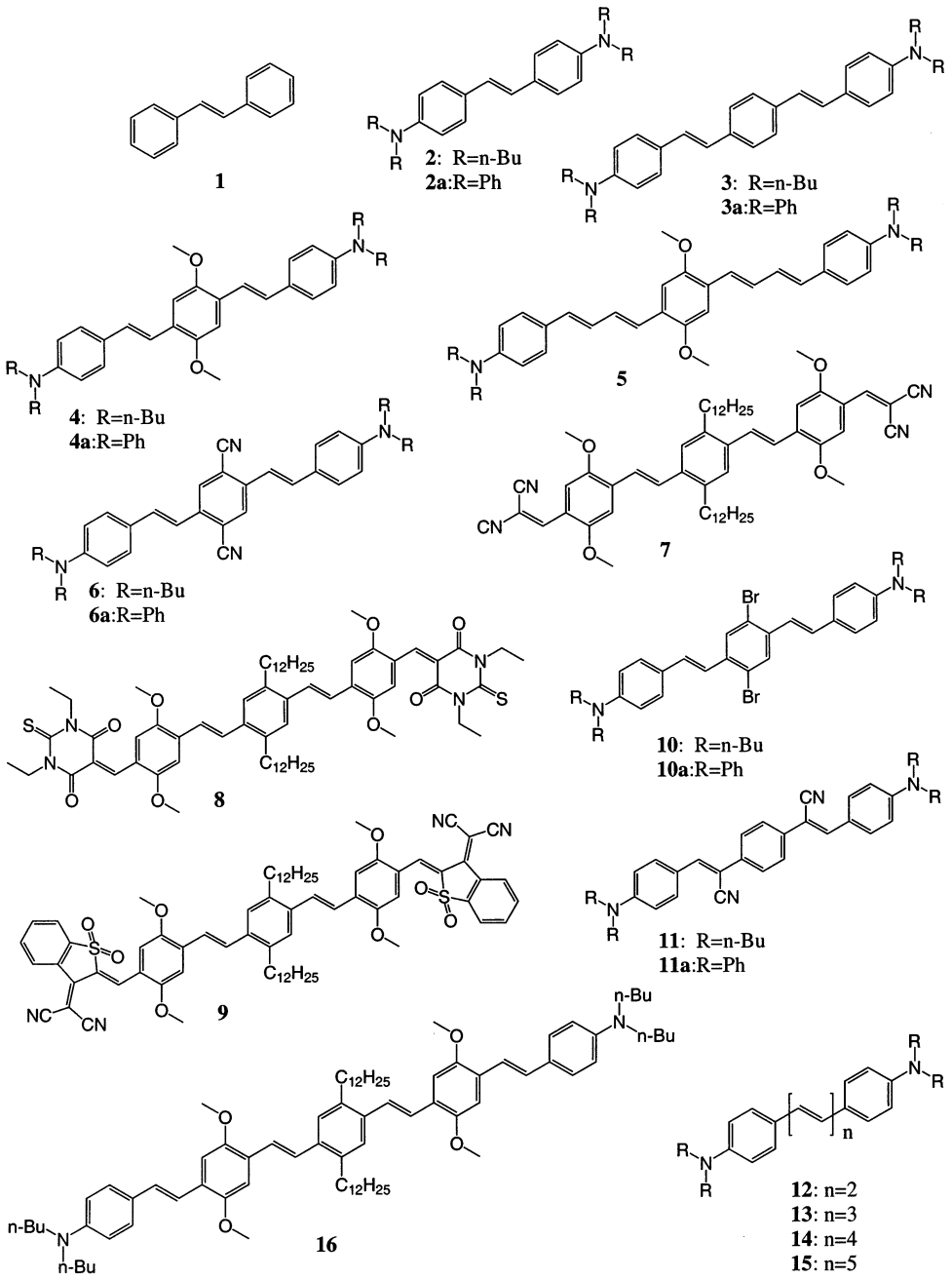

Figure 1. Molecules studied in this paper.

be underestimated. This is why special treatment, such as low-temperature experiments[54] and partial positional occupational refinements,[55] is needed. After precautions are taken, the BLA in the crystal is 0.136−0.146 Å, and nonplanarity is 5°. One may argue that the crystal environment distorts the molecular geometry from the gas-phase value, but we have to keep in mind that the spectroscopic experiments are done in solution with the polarity similar to that in stilbene crystal. Gas-phase electron diffraction of the *trans*-stilbene[56] yields a similar BLA of 0.152 Å, but nonplanarity is found to be much greater (32°). However, this result can be ambiguously interpreted as a mean amplitude of the torsional motion in the soft single-well potential, or as a minimum of a double-well potential. An indirect evidence for the planarity of stilbene in solution was presented recently.[52] Although the barrier to planarization at the MP2/6-31G* level was found to be 0.8 kcal/mol, comparison of the predicted vibrational spectra with experiment in solution revealed the agreement with the planar model.

Steric effect of the substituents destabilizes planar geometry, while the resonance effect stabilizes it. Our HF calculations predict planar geometry for the compounds **12**−**15** (Figure 1), which have longer conjugated chains between the phenyl rings. For the rest of the molecules, the barrier to planarization is less than 1 kcal/mol. The only exceptions are **9** and **11**, where these barriers are 4.7 and 25.1 kcal/mol, respectively. Coincidentally, these are the only nonplanar molecules produced by the DFT optimization. A greater planarization barrier for molecule **11** was expected from the significant nonplanarity of molecule **11a** in the crystal.[18] However, the experimental two-photon cross section, which is sensitive to molecular planarity, has comparable values for molecules **11** and **4**. This could be rationalized as evidence of a similar degree of nonplanarity for these molecules in solution.

Regardless of the optimum value of the torsional angle, we can conclude that the torsional potential in stilbene and its analogues is shallow and that the molecules adopt a wide range

TABLE 1: Calculated and Experimental Torsional Angles (deg) and Bond-Length Alternation (Å) in the Vinyl Bridge Adjacent to the Central Ring in the Molecules 1, 6a, and 11a[a]

compound, method	C—C	C═C	BLA	torsion
1, gas[56]	1.481	1.329	0.152	32.5
1, crystal[54]	1.472	1.336	0.136	5.2
1, crystal[55]	1.471	1.326	0.145	5.3
1, AM1	1.453	1.343	0.110	22.9
1, HF/6-31G	1.475	1.332	0.143	21.5
1, B3LYP/6-31G	1.468	1.352	0.116	0
1, MP2/6-31G	1.482	1.364	0.118	33.3
6a, crystal[18]	1.467	1.328	0.139	24.3
6a, AM1	1.452	1.345	0.107	26.7
6a, HF/6-31G	1.471	1.334	0.137	25.2
6a, HF/6-31G	1.470	1.335	0.135	24.3
6a, B3LYP/6-31G	1.458	1.357	0.101	1.6
6a, MP2/6-31G	1.471	1.367	0.104	27.0
11a, crystal[18]	1.478	1.353	0.125	43.2
11a, AM1	1.466	1.352	0.114	36.9
11a, HF/6-31G	1.490	1.343	0.147	35.9
11a, HF/6-31G	1.492	1.346	0.146	36.1
11a, B3LYP/6-31G	1.488	1.371	0.117	24.8
11a, MP2/6-31G	1.491	1.376	0.115	35.9

[a] BLA is defined as BLA = r(C—C) − r(C═C).

of torsional angles in solution at room temperature. For this reason, we carry the calculations at both planar and nonplanar optimal geometry.

Our geometry optimization results are summarized in Table 1. For the molecules **1**, **6a**, and **11a**, HF gives the best agreement with experiment[18,54−56] for the BLA values compared to B3LYP, AM1, and MP2 geometries. As it often happens, errors due to an incomplete basis set cancel the errors due to the neglect of electron correlation. Systematic underestimation of the BLA parameter by DFT methods (especially in pure DFT) was discussed recently.[57] Another evidence of overdelocalization in conjugated systems in DFT methods is demonstrated by overestimation of the rotation barriers around single bonds.[58] All methods fail to reproduce the relative order in the BLA values between **6a** and **11a**. One may attribute this failure to the neglected effect of the crystal environment.

B. OPA and TPA Transition Frequencies. The results of our TDDFT calculations and related experimental data are presented in Tables 2 and 3, and the summary is shown in Figure 2. For TDDFT/B3LYP calculations, we used three sets of input geometries optimized with (i) the B3LYP functional to provide a consistent treatment within the same DFT approach for both ground and excited-state properties, (ii) the HF method (denoted HF/nonplanar), and (iii) the HF method with the planar constraint (denoted HF/planar). The last two methods provide the best agreement with experimental crystal data for molecular geometries (see discussion in the previous section).

Assuming that the molecules (Figure 1) belong to the C_{2h} symmetry group, electronic states with B_u and A_g symmetries are allowable in the OPA and TPA spectra, respectively. In the majority of cases, the most intense OPA state is the first singlet excited state S1 and the TPA state is S2. For the molecules **1** and **14**, the TPA state is S4, and for some molecules there are two (S2 and S6 for compound **7** and S2 and S4 for compound **10**) or three (S2, S4, and S6 for compound **4** and S2, S3, and S6 for compound **9**) TPA states. Molecule **6** has two OPA (S1 and S3) and two TPA (S2 and S4) states. Subsequently, molecules **4**, **7**, and **10** have a second satellite peak in their calculated TPA spectra, and molecule **6** has three maxima of comparable height. The second maximum in the TPA spectrum of compound **7** was indeed observed in experiment.[17] Tables 2 and 3 and Figure 2 show the OPA and TPA transition frequencies corresponding to the most intense maxima in the respective spectra.

TABLE 2: Calculated and Experimental[16−18] Frequencies (eV) Corresponding to the OPA Maxima (Usually the Lowest Excited State of B_u Symmetry) of Molecules Shown in Figure 1[a]

compound	exp	B3LYP	HF/nonplanar	HF/planar
1	4.18	4.07	4.34	4.23
2	3.32	3.46	3.67	3.61
2a	3.20		3.20	
3	3.04	2.89	3.15	3.06
3a	3.02		2.95	
4	2.90	2.76	3.04	2.93
4a	2.91		2.91	
5	2.72	2.52	2.74	2.73
6	2.53	2.49	2.67	2.65
6a	2.63		2.54	
7	2.42	2.22	2.35	2.36
8	2.24	2.00	2.14	2.11
9	2.01	1.62	1.68	1.71
10		2.75	2.90	2.97
10a	2.92		2.78	
11	2.83	2.80	3.07	2.86
11a	2.82		2.84	
12	3.18	3.14	3.32	3.32
13	3.01	2.88	3.08	3.08
14	2.88	2.66	2.89	2.89
15	2.76	2.48	2.73	2.73
16	2.65	2.36	2.55	2.60

[a] Calculations have been done at the TDDFT/B3LYP level using three different optimized geometry sets (B3LYP, HF/planar, and HF/nonplanar).

TABLE 3: Calculated and Experimental[16−18] Frequencies (eV) Corresponding to the TPA Maxima (half energy of an excited state of A_g Symmetry Active in TPA) of Molecules Shown in Figure 1[a]

compound	exp	B3LYP	HF/nonplanar	HF/planar
1	2.41	2.60	2.69	2.67
2	2.05	2.13	2.19	2.18
2a	1.80		1.80	
3	1.70	1.69	1.79	1.77
3a	1.66		1.62	
4	1.70	1.65	1.77	1.73
4a	1.66		1.62	
5	1.60	1.47	1.58	1.57
6	1.50	1.46	1.52	1.50
6a	1.49		1.38	
7	1.50	1.52	1.65	1.56
8	1.28	1.15	1.21	1.19
9	1.27	1.25	1.21	1.24
10		1.60	1.69	1.66
10a	1.55		1.52	
11	1.57	1.55	1.68	1.62
11a	1.50		1.55	
12	1.94	1.91	1.98	1.98
13	1.75	1.73	1.82	1.82
14	1.70	1.59	1.69	1.69
15	1.70	1.47	1.59	1.59
16	1.48	1.34	1.46	1.43

[a] Calculations have been done at the TDDFT/B3LYP level using three different optimized geometry sets (B3LYP, HF/planar, and HF/nonplanar).

The B3LYP geometries systematically underestimate calculated transition energies compared to experiment in both OPA and TPA spectra (see Figure 2). We attribute this to the underestimated BLA parameters in the B3LYP-optimized geometries (section 4.1) which results in overestimated electronic delocalization and subsequently in redshifts for the excited-state energies.

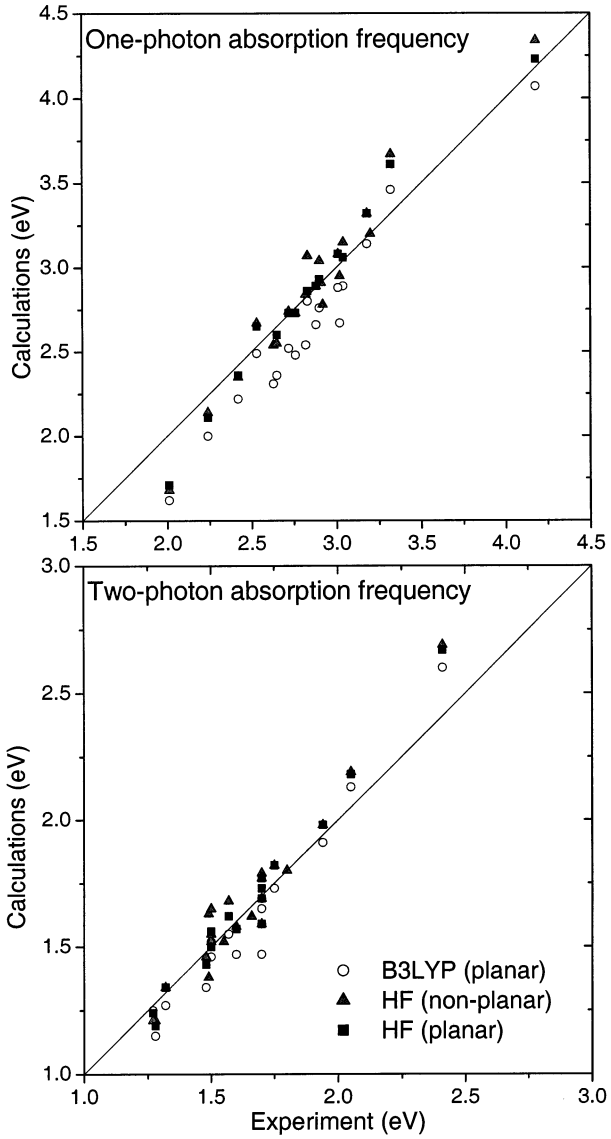

Figure 2. Comparison of calculated and experimental[16−18] frequencies corresponding to the OPA (top panel) and TPA (bottom panel) maxima of molecules shown in Figure 1. Calculations have been done at the TDDFT/B3LYP level using three different optimized geometry sets (B3LYP, HF/planar, and HF/nonplanar).

In contrast, our calculations based on the HF geometries, which agree with crystallographic data, result in the excited-state energies consistent with experiment. Even though the nonplanarity leads to weak blueshifts in the excitation energies, this effect is small, and the OPA and TPA frequencies obtained using HF/planar and HF/nonplanar geometries both agree well with experiment. Compound **9** has very strong acceptor substituents. Subsequently, its electronic spectrum is a complex superposition of delocalized and charge-transfer transitions.[59] For this molecule, we observe significant deviations from experiment for the OPA transition frequency and TPA cross section (section 4.3), which may be partially attributed to the strong solvent effects that are not accounted for in the present study.

Overall, TDDFT provides an excellent agreement with experiment for *both* OPA and TPA excitation frequencies across the entire set of molecules. For the two-photon transition energies, the mean absolute errors are 0.06, 0.064, and 0.08 eV (3.8, 4.1, and 4.6%) at HF/planar, HF/nonplanar, and B3LYP geometries, respectively. For the one-photon absorption, the mean errors in the transition energy are 0.09, 0.11, and 0.2 eV (3.1, 3.9, and 6.9%) for these geometries.

C. TPA Cross Sections. Comparison with experiment of calculated TPA cross sections is a challenging problem. The standard methodology, for example, exists for the OPA spectra, where an integrated intensity for each peak in the linear absorption spectrum gives the oscillator strength for a particular optical transition. The oscillator strengths can also be directly evaluated in the theoretical simulations using calculated transition dipoles and frequencies.[60] Similar techniques are yet to be developed for TPA spectroscopies.[61] To simulate the finite line widths in the experimental TPA spectra mediated by inhomogenious broadening caused by temperature and solvent effects, we introduce an empirical damping factor Γ for all molecules and for all excited states by replacing the transition frequencies Ω_ν with $(\Omega_\nu - i\Gamma)$ in the denominators of eqs 2.4−2.11. The average line width $\Gamma = 0.1$ eV for a given family of molecules was suggested in an experimental study.[17] The line-broadening parameter Γ has a significant effect on the calculated TPA cross sections. Subsequently, the comparison with experiment cannot be done objectively in the present study; however, we examine the emerging trends.

We have calculated the TPA cross sections with eqs 2.1−2.11 using the TDDFT/B3LYP approach and optimized HF/planar geometries. To identify the dominating terms in the expansion we compared (i) complete calculations (except terms containing $v^{(2)}$ and $v^{(3)}$), (ii) calculations that neglect the Coulomb operators on the cross densities $\tilde{V}((1/2)((\xi_\beta, \bar{\rho}),\xi_\alpha))$ (this approximation can speed up the TPA computations considerably), and (iii) calculations which neglect Coulomb terms V altogether to test the effect of couplings related to the Coulomb exchange-correlation interactions compared to the dipole-mediated couplings (denoted as dipole approximation). The TPA cross sections were computed using six singlet excited states for each of the molecules studied. A small number of excited states should be sufficient for computation of the resonance responses where only the electronic states with energies close to the resonance frequency provide substantial contributions. Increasing the number of calculated excited states from 6 to 30 for molecules **1** and **12** changes the resulting cross sections by about 10%.

Examples of calculated and measured[17] spectra are given in Figure 3 for molecules **15** (OPA) and **16** (TPA). Experimental linear absorption spectrum has well-pronounced vibronic progression that is not accounted for in the present calculations but may be computed using optimal ground and excited-state geometries and a set of normal modes.[62,63] In contrast, distinct peaks in TPA spectra usually reflect involvement of different excited states.[61]

Experimental and calculated cross section magnitudes at the absolute maxima of TPA spectra are summarized in Table 5, and plotted in Figure 4. As expected, the agreement of calculations and experiment is far from being perfect, and the deviations are not systematic. Overall the calculated cross sections follow the experimental trend, except for unsubstituted stilbene, where the calculated value deviates from experiment by an order of magnitude. This failure may be attributed to unusually strong double-excitation character of the two-photon excited state in unsubstituted oligomers (e.g., polyenes),[50] which is not reproduced by the conventional implementations of TDDFT.[64] We note that the terms involving the Coulomb operators on cross densities are virtually negligible and the results of full calculations (i) coincide with (ii) the approximation

TABLE 4: Calculated and Experimental[16−18] Frequencies (eV) and TPA Cross Sections (GM, in Parentheses) as a Function of the Basis-Set Size[a]

compound	exp	STO-3G	6-31G	6-31G*	6-31+G*	6-311G
1 planar	2.41(12)	3.05(91)	2.68(186)	2.64(109)	2.56(115)	2.60(108)
1 nonplanar	2.41(12)	3.06(81)	2.68(153)	2.64(94)	2.57(100)	2.67(99)
2	2.05(200)	2.44(200)	2.18(218)	2.18(225)	2.11(213)	2.15(255)
3	1.70(995)	1.99(452)	1.77(780)	1.76(781)	1.72(1207)	1.73(1234)
12	1.94(260)	2.19(303)	1.97(385)	1.97(386)	1.94(663)	1.95(412)
13	1.75(320)	2.01(433)	2.11(537)	1.81(546)	1.78(608)	1.80(557)

[a] Calculations have been done at the TDDFT/B3LYP level for molecules **1** (in both HF/planar and HF/nonplanar geometry), **2**, **3**, **12**, **13**.

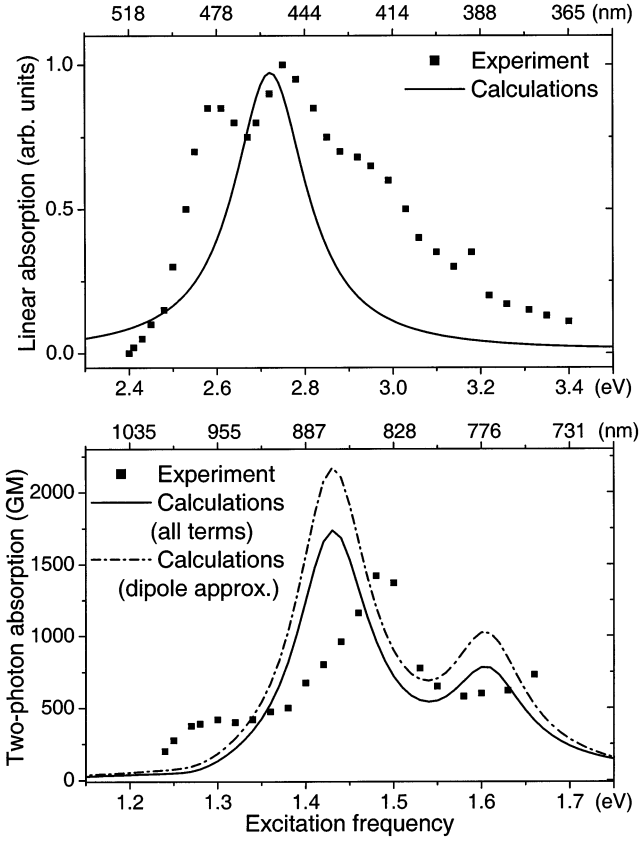

Figure 3. Comparison of calculated and experimental[17] OPA (top panel) and TPA (bottom panel) spectra for molecules **15** and **16**, respectively.

(the latter results are not shown in Table 5 and Figure 4). In contrast, the other terms related to the Coulomb exchange-correlation interactions make a significant difference in the TPA magnitudes (up to 20−50%) and need to be accounted for the cross section calculations. A detailed analysis of the dominant contributions (related to the Liouville space paths) to the resonant and off-resonant third-order optical responses will be published elsewhere.

It is worth noting that the TPA cross sections at the HF/planar geometry are typically 20−40% greater than those of the HF/nonplanar geometry (the latter results are not shown), which indicates a strong dependence of the TPA intensities on molecular conformations. The largest deviations from the experimental cross sections (3- and 2-fold for the molecules **6** and **9**, respectively) are probably caused by experimentally unresolved multiple maxima, as the TPA intensities for those molecules are distributed over the multiple states. We also expect TPA intensities to depend on the solvent effects, which are not accounted for in the present study. Ambiguity in the choice of the damping factor Γ can be another reason for the deviations from experiment.

TABLE 5: Calculated and Experimental[16−18] TPA Cross Sections (GM) of Molecules Shown in Figure 1[a]

compound	exp	all terms	dipole approx
1	12	454	164
2	200	379	341
2a	190		
3	995	779	1075
3a	805		
4	900	1145	1043
4a	855		
5	1250	960	1288
6	1750	650	585
6a	1640		
7	620	1180	1501
8	1750	1546	1943
9	4400	2230	2915
10		845	928
10a	450		
11	890	729	661
11a	730		
12	260	386	633
13	320	536	875
14	425	765	1304
15	1300	1180	1873
16	1420	1736	2173

[a] Calculations have been done at the TDDFT/B3LYP level using HF/Planar-optimized geometries and $\Gamma = 0.1$ eV empirical line widths for all molecules.

It was shown recently that the calculated values of the dipole moments for the excited states of small molecules (such as pyrrole and furan) strongly depend on the choice of the basis set and density functional used.[65] One would expect similar dependence for the transition dipole moments as well. However, calculated TPA for the five smallest molecules of the set, presented in Table 4, does not indicate significant basis-set dependence. The change upon addition of polarization and diffuse functions, and from double to triple-ζ basis, is only marginal (unsubstituted stilbene is an exception again). The minimal basis set (STO-3G) somewhat decreases the calculated TPA values, which often improves the agreement with experiment (even though the agreement with excitation energies worsens). This conclusion seems to contradict the well-established fact (see ref 66 for discussion), that specifically designed polarization functions may significantly improve the response properties. To rationalize this fact, we recall that TPA of molecules in question originates from the response of mobile π electrons strongly delocalized over the conjugated chains, and contribution of the atomic polarization is minimal. That is why polarization functions in our study almost have no effect on the TPA spectra. In conjugated systems, the minimal basis tends to effectively localize the electrons, which are overdelocalized in the DFT description. The detailed investigation on the best choice of the density functional and the basis set for calculations of nonlinear optical responses will be published elsewhere. However, the absolute errors in the TPA cross sections at the

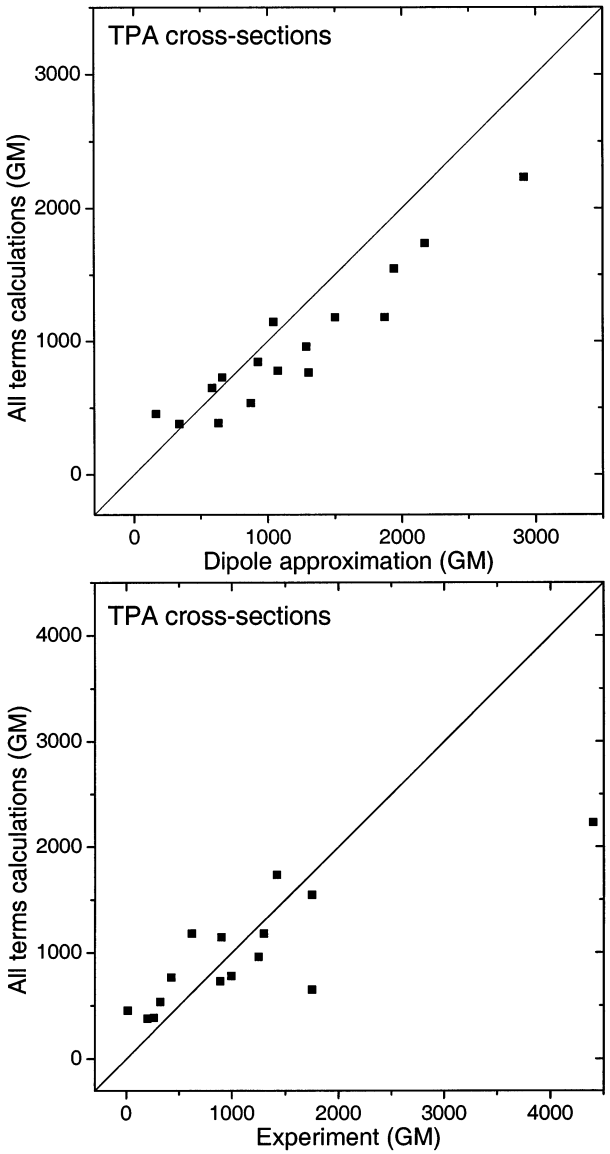

Figure 4. Comparison of full vs dipole-approximation calculations (top panel) and calculated vs experimental[16−18] (bottom panel) TPA cross sections of molecules shown in Figure 1. Calculations have been done at the TDDFT/B3LYP level using HF/planar-optimized geometries and $\Gamma = 0.1$ eV empirical line widths for all molecules.

TDDFT/B3LYP/6-31G level are already comparable with the best literature values.[16−18]

V. Conclusions

It is well known that $\pi-\pi^*$ excited states in polyconjugated molecules are highly correlated and, in principle, require a comprehensive CI treatment for their correct description.[67] However, this method is computationally expensive even at the semiempirical level and even for small molecules. Additionally, a truncation to the reduced set of electronic configurations may introduce imbalance between ground- and excited-state correlation descriptions[68] and size-consistency problems.[21,22] This is especially evident for centrosymmetric molecules, where the OPA states have B_u symmetry and could be easily described with the single excitations, while the TPA states have A_g symmetry (same as the ground state) and require double excitations for their correct description. Including double excitations, however, may overcorrelate the ground state. That is why semiempirical methods (such as ZINDO), parametrized to reproduce OPA spectra with the single CI, fail to describe the TPA states, and methods designed to reproduce the TPA spectra (such as MRD-CI) may introduce errors in the linear spectra description.

TDDFT includes electronic correlations implicitly through an underlying density functional and thus presents the balanced treatment for ground and excited states. However, the exact density functional is unknown, and the current implementations are limited to the adiabatic version of TDDFT.[26,48] Nevertheless, the TDDFT approach presents a great improvement over the TDHF and CIS results[69] and currently became a method of choice for computing excited states in extended molecules.[26,32,70−72]

In this study, one- and two-photon-absorption spectra are calculated at the TDDFT/B3LYP/6-31G level for the series of stilbene and bis(styryl)benzene derivatives. Instead of the habitual SOS approach, the actual third-order response formula for the time-dependent responses is used.[39] On average, both TPA and OPA transition energies are predicted with better than 4% accuracy, which presents a considerable improvement over semiempirical and ab initio calculations found in the literature. As one can see, TDDFT reproduces OPA and TPA excitation energies equally well. Usually this is not the case for other computational methods. In addition, calculated TPA cross sections follow the experimental trend as well, given the large amount of uncertainty introduced by an empirical broadening which makes the quantitative comparison of the cross sections with experiment impossible. Nevertheless, the predicted TPA cross sections are among the best found in the literature.

It was found that using line widths derived from experimental data considerably improves the agreement between the calculated and experimental TPA cross sections.[61] However, the quantitative comparison with experiment is still a subject for the future studies toward computing the absolute magnitudes of the TPA cross sections when the chromophore's vibronic structures and interactions with the solvent are explicitly accounted for.

VI. Acknowledgments

The authors of this paper would like to thank Dr. Richard L. Martin and Dr. Mike Frisch for fruitful discussions and their help with the Gaussian 98 code and Dr. Rudolph Magyar for his help with the manuscript. The research at Los Alamos National Laboratory is supported by the Laboratory Research and Development program of the U.S. Department of Energy. This support is gratefully acknowledged.

References and Notes

(1) Bhawalkar, J. D.; He, G. S.; Prasad, P. N. *Rep. Prog. Phys.* **1996**, *59*, 1041.

(2) Joshi, M. P.; Pudavar, H. E.; Swiatkiewicz, J.; Prasad, P. N.; Reianhardt, B. A. *Appl. Phys. Lett.* **1999**, *74*, 170.

(3) Cumpston, B. H.; Ananthavel, S. P.; Barlow, S.; Dyer, D. L.; Ehrlich, J. E.; Erskine, L. L.; Heikal, A. A.; Kuebler, S. M.; Lee, I. Y. S.; McCord-Maughon, D.; Qin, J. Q.; Rockel, H.; Rumi, M.; Wu, X. L.; Marder, S. R.; Perry, J. W. *Nature* **1999**, *398*, 51.

(4) Shen, Y. Z.; Swiatkiewicz, J.; Jakubczyk, D.; Xu, F. M.; Prasad, P. N.; Vaia, R. A.; Reinhardt, B. A. *Appl. Opt.* **2001**, *40*, 938.

(5) Pudavar, H. E.; Joshi, M. P.; Prasad, P. N.; Reinhardt, B. A. *Appl. Phys. Lett.* **1999**, *74*, 1338.

(6) Kawata, S.; Kawata, Y. *Chem. Rev.* **2000**, *100*, 1777.

(7) Spangler, C. W. *J. Mater. Chem.* **1999**, *9*, 2013.

(8) Bauer, C.; Schnabel, B.; Kley, E. B.; Scherf, U.; Giessen, H.; Mahrt, R. F. *Adv. Mater.* **2002**, *14*, 673.

(9) Konig, K.; *J. Microsc. (Oxford)* **2000**, *200*, 83.

(10) Zipfel, W. R.; Williams, R. M.; Christie, R.; Nikitin, A. Y.; Hyman, B. T.; Webb, W. W. *Proc. Natl. Acad. Sci. U. S. A.* **2003**, *100*, 7075.

(11) Fisher, A. M. R.; Murphree, A. L.; Gomer, C. J. *Lasers Surg. Med.* **1995**, *17*, 2.
(12) Xu, C.; Zipfel, W.; Shear, J. B.; Williams, R. M.; Webb, W. W. *Proc. Natl. Acad. Sci. U. S. A.* **1996**, *93*, 10763.
(13) Heikal, A. A.; Huang, S. H.; Halik, M.; Marder, S. R.; Wenseleers, W.; Perry, J. W.; Webb, W. W. *Biophys. J.* **2002**, *82*, 493A.
(14) Reinhardt, B. A.; Brott, L. L.; Clarson, S. J.; Dillard, A. G.; Bhatt, J. C.; Kannan, R.; Yuan, L. X.; He, G. S.; Prasad, P. N. *Chem. Mater.* **1998**, *10*, 1863.
(15) Baur, J. W.; Alexander, M. D.; Banach, M.; Denny, L. R.; Reinhardt, B. A.; Vaia, R. A.; Fleitz, P. A.; Kirkpatrick, S. M. *Chem. Mater.* **1999**, *11*, 2899.
(16) Albota, M.; Beljonne, D.; Brédas, J. L.; Ehrlich, J. E.; Fu, J. Y.; Heikal, A. A.; Hess, S. E.; Kogej, T.; Levin, M. D.; Marder, S. R.; McCord-Maughon, D.; Perry, J. W.; Rockel, H.; Rumi, M.; Subramaniam, C.; Webb, W. W.; Wu, X. L.; Xu, C. *Science* **1998**, *281*, 1653.
(17) Rumi, M.; Ehrlich, J. E.; Heikal, A. A.; Perry, J. W.; Barlow, S.; Hu, Z. Y.; McCord-Maughon, D.; Parker, T. C.; Rockel, H.; Thayumanavan, S.; Marder, S. R.; Beljonne, D.; Bredas, J. L. *J. Am. Chem. Soc.* **2000**, *122*, 9500.
(18) Pond, S. J. K.; Rumi, M.; Levin, M. D.; Parker, T. C.; Beljonne, D.; Day, M. W.; Bredas, J. L.; Marder, S. R.; Perry, J. W. *J. Phys. Chem. A* **2002**, *106*, 11470.
(19) Mukamel, S. *Principles of Nonlinear Optical Spectroscopy*; Oxford: New York, 1995.
(20) Rodenberger, D. C.; Heflin, J. R.; Garito, A. F. *Nature* **1992**, *359*, 309.
(21) Heflin, J. R.; Wong, K. Y.; Zamanikhamiri, O.; Garito, A. F. *Phys. Rev. B* **1988**, *38*, 1573.
(22) Yaron, D. *Phys. Rev. B* **1996**, *54*, 4609.
(23) Tretiak, S.; Mukamel, S. *Chem. Rev.* **2002**, *102*, 3171.
(24) Norman, P.; Luo, Y.; Agren, H. *Opt. Commun.* **1999**, *168*, 297.
(25) Wang, C. K.; Macak, P.; Luo, Y.; Agren, H. *J. Chem. Phys.* **2001**, *114*, 9813.
(26) Casida, M. E. In *Recent Advances in Density-Functional Methods, Part I*; Chong, D. A., Ed.; World Scientific: Singapore, 1995; Vol. 3.
(27) Fabian, J.; Diaz, L. A.; Seifert, G.; Niehaus, T. *THEOCHEM* **2002**, *594*, 41.
(28) Handy, N. C.; Tozer, D. J. *J. Comput. Chem.* **1999**, *20*, 106.
(29) Andreu, R.; Garin, J.; Orduna, J. *Tetrahedron* **2001**, *57*, 7883.
(30) Hirata, S.; Head-Gordon, M.; Bartlett, R. J. *J. Chem. Phys.* **1999**, *111*, 10774.
(31) Casida, M. E.; Salahub, D. R. *J. Chem. Phys.* **2001**, *113*, 8918.
(32) Bauernschmitt, R.; Ahlrichs, R. *Chem. Phys. Lett.* **1996**, *256*, 454.
(33) Furche, F. *J. Chem. Phys.* **2001**, *114*, 5982.
(34) Salek, P.; Vahtras, O.; Helgaker, T.; Agren, H. *J. Chem. Phys.* **2002**, *117*, 9630.
(35) van Gisbergen, S. J. A.; Snijders, J. G.; Baerends, E. J. *J. Chem. Phys.* **1998**, *109*, 10644.
(36) Salek, P.; Vahtras, O.; Guo, J. D.; Luo, Y.; Helgaker, T.; Agren, H. *Chem. Phys. Lett.* **2003**, *374*, 446.
(37) Chernyak, V.; Mukamel, S. *J. Chem. Phys.* **2000**, *112*, 3572.
(38) Larsen, H.; Jorgensen, P.; Olsen, J.; Helgaker, T. *J. Chem. Phys.* **2000**, *113*, 8908.
(39) Tretiak, S.; Chernyak, V. *J. Chem. Phys.* **2003**, *119*, 8809.
(40) Das, G. P.; Yeates, A. T.; Dudis, D. S. *Chem. Phys. Lett.* **2002**, *361*, 71.
(41) Zhou, X.; Ren, A. M.; Feng, J. K.; Liu, X. J. *J. Phys. Chem. A* **2003**, *107*, 1850.
(42) Garito, A. F.; Heflin, J. R.; Wong, K. Y.; Zamani-Khamiri, O. In *Organic Materials for Nonlinear Optics*; Hann, R. A., Bloor, D., Ed.; Royal Chemical Society, Burlington House: New York, 1989.
(43) Orr, B. J.; Ward, J. F. *Mol. Phys.* **1971**, *20*, 513.
(44) Kogej, T.; Beljonne, D.; Meyers, F.; Perry, J. W.; Marder, S. R.; Bredas, J. L. *Chem. Phys. Lett.* **1998**, *298*, 1.
(45) Becke, A. D. *J. Chem. Phys.* **1993**, *98*, 5648.
(46) Becke, A. D. *J. Chem. Phys.* **1993**, *98*, 1372.
(47) Furche, F.; Ahlrichs, R. *J. Chem. Phys.* **2002**, *117*, 7433.
(48) Frisch, M. J.; Trucks, G. W.; Schlegel, H. B.; Scuseria, G. E.; Robb, M. A.; Cheeseman, J. R.; Zakrzewski, V. G.; Montgomery, J. A., Jr.; Stratmann, R. E.; Burant, J. C.; Dapprich, S.; Millam, J. M.; Daniels, A. D.; Kudin, K. N.; Strain, M. C.; Farkas, O.; Tomasi, J.; Barone, V.; Cossi, M.; Cammi, R.; Mennucci, B.; Pomelli, C.; Adamo, C.; Clifford, S.; Ochterski, J.; Petersson, G. A.; Ayala, P. Y.; Cui, Q.; Morokuma, K.; Malick, D. K.; Rabuck, A. D.; Raghavachari, K.; Foresman, J. B.; Cioslowski, J.; Ortiz, J. V.; Stefanov, B. B.; Liu, G.; Liashenko, A.; Piskorz, P.; Komaromi, I.; Gomperts, R.; Martin, R. L.; Fox, D. J.; Keith, T.; Al-Laham, M. A.; Peng, C. Y.; Nanayakkara, A.; Gonzalez, C.; Challacombe, M.; Gill, P. M. W.; Johnson, B. G.; Chen, W.; Wong, M. W.; Andres, J. L.; Head-Gordon, M.; Replogle, E. S.; Pople, J. A. *Gaussian 98*, revision A.11; Gaussian, Inc.: Pittsburgh, PA, 1998.
(49) Marder, S. R.; Perry, J. W.; Tiemann, B. G.; Gorman, C. B.; Gilmour, S.; Biddle, S. L.; Bourhill, G. *J. Am. Chem. Soc.* **1993**, *115*, 2524.
(50) Zojer, E.; Beljonne, D.; Kogej, T.; Vogel, H.; Marder, S. R.; Perry, J. W.; Bredas, J. L. *J. Chem. Phys.* **2002**, *116*, 3646.
(51) Zalesny, R.; Bartkowiak, W.; Styrcz, S.; Leszczynski, J. *J. Phys. Chem. A* **2002**, *106*, 4032.
(52) Choi, C. H.; Kertesz, M. *J. Phys. Chem. A* **1997**, *101*, 3823.
(53) Harada, J.; Ogawa, K. *J. Am. Chem. Soc.* **2001**, *123*, 10884.
(54) Hoekstra, A.; Meertens, P.; Vos, A. *Acta Crystallogr. B* **1975**, *31*, 2813.
(55) Bouwstra, J. A.; Schouten, A.; Kroon, J. *Acta Crystallogr. C* **1984**, *40*, 428.
(56) Traetteberg, M.; Frantsen, E. B.; Mijlhoff, F. C.; Hoekstra, A. *J. Mol. Struct.* **1975**, *26*, 57.
(57) Choi, C. H.; Kertesz, M.; Karpfen, A. *J. Chem. Phys.* **1997**, *107*, 6712.
(58) Karpfen, A.; Choi, C. H.; Kertesz, M. *J. Phys. Chem. A* **1997**, *101*, 7426.
(59) Tretiak, S.; Chernyak, V.; Mukamel, S. *J. Am. Chem. Soc.* **1997**, *119*, 11408.
(60) Herzberg, G. In *Molecular Spectra and Molecular Structure. I. Spectra of Diatomic Molecules*; Zyss, J., Chemla, D. S., Ed.; Van Nostrand Reinhold Company: New York, 1950; Vol. 2.
(61) Bartholomew, G. P. Rumi, M.; Pond, S. J. K.; Perry, J. W.; Tretiak, S.; Bazan, G. C., to be published.
(62) Cornil, J.; Beljonne, D.; Heller, C. M.; Campbell, I. H.; Laurich, B. K.; Smith, D. L.; Bradley, D. D. C.; Mullen, K.; Brédas, J. L. *Chem. Phys. Lett.* **1997**, *278*, 139.
(63) Tretiak, S.; Saxena, A.; Martin, R.; Bishop, A. *Phys. Rev. Lett.* **2002**, *8909*, 7402.
(64) Appel, H.; Gross, E. K. U.; Burke, K. *Phys. Rev. Lett.* **2003**, *90*, 043005.
(65) Burcl, R.; Amos, R. D.; Handy, N. C. *Chem. Phys. Lett.* **2002**, *355*, 8.
(66) Chong, D. L. P.; Gruning, M.; Baerends, E. J. *J. Comput. Chem.* **2003**, *24*, 1582.
(67) Ramasesha, S.; Soos, Z. G. *J. Chem. Phys.* **1984**, *80*, 3278.
(68) Ohmine, I.; Karplus, M.; Schulten, K. *J. Chem. Phys.* **1978**, *68*, 2298.
(69) Hsu, C. P.; Hirata, S.; Head-Gordon, M. *J. Phys. Chem. A* **2001**, *105*, 451.
(70) Stratmann, R. E.; Scuseria, G. E.; Frisch, M. J. *J. Chem. Phys.* **1998**, *109*, 8218.
(71) Bauernschmitt, R.; Ahlrichs, R.; Hennrich, F. H.; Kappes, M. M. *J. Am. Chem. Soc.* **1998**, *120*, 5052.
(72) Wiberg, K. B.; Stratmann, R. E.; Frisch, M. J. *Chem. Phys. Lett.* **1998**, *297*, 60.